

# Interaction Visual Transformer for Egocentric Action Anticipation

Debaditya Roy<sup>1</sup>, Ramanathan Rajendiran<sup>1</sup>, and Basura Fernando<sup>1,2</sup>

<sup>1</sup>Institute of High Performance Computing (IHPC), Agency for Science, Technology and Research (A\*STAR), 1 Fusionopolis Way, #16-16 Connexis, Singapore 138632, Republic of Singapore.

<sup>2</sup>Centre for Frontier AI Research (CFAR), Agency for Science, Technology and Research (A\*STAR), 1 Fusionopolis Way, #16-16 Connexis, Singapore 138632, Republic of Singapore

## Abstract

Human-object interaction is one of the most important visual cues and we propose a novel way to represent human-object interactions for egocentric action anticipation. We propose a novel Transformer variant to model interactions by computing the change in the appearance of objects and human hands due to the execution of the actions and use those changes to refine the video representation. Specifically, we model interactions between hands and objects using Spatial Cross-Attention (SCA) and further infuse contextual information using Trajectory Cross-Attention to obtain environment-refined interaction tokens. Using these tokens, we construct an interaction-centric video representation for action anticipation. We term our model InAViT which achieves state-of-the-art action anticipation performance on large-scale egocentric datasets EPICKTICHENS100 (EK100) and EGTEA Gaze+. InAViT outperforms other visual transformer-based methods including object-centric video representation. On the EK100 evaluation server, InAViT is the top-performing method on the public leaderboard (at the time of submission) where it outperforms the second-best model by 3.3% on mean-top5 recall.

## 1 Introduction

Egocentric action anticipation is crucial for developing AI assistants for surgery [53], assembly [7], and construction [54]. Egocentric action anticipation is also becoming a viable technology thanks to wide use of wearable cameras such as GoPro [34]. In egocentric action anticipation, the model predicts the immediate action that is going to happen, usually 1 second into the future [13]. However, the observed video may not contain sufficient visual cues and semantics to predict the future actions accurately. Therefore, it is important to leverage all available information when predicting future actions. It is well known that relationships between objects and humans indicate the actions humans are executing. A recent line of work explored these properties for effective action recognition [41] and action anticipation [47]. We propose to exploit the contextual visual changes in humans and objects during an interaction to boost anticipation. This type of visual information is significant for action anticipation. For example, when standing in front of the sink, *putting down a used pan* or *opening the tap* are probable future actions. In this instance, the likely future action depends on whether the observed interaction is *servicing food from a pan* or *picking up a glass* as shown in Fig. 1. Therefore, we propose to model the interactions between hands and objects using a novel visual transformer model where the attention weights determine informative interactions for predicting the next action.

More specifically, the human hands contribute more to the visual change of the interacting object(s) in egocentric videos [10, 8]. Similarly, the appearance of the hand is affected mostly by the interacting objects. For example, a spoon’s appearance is different when it is used for feeding

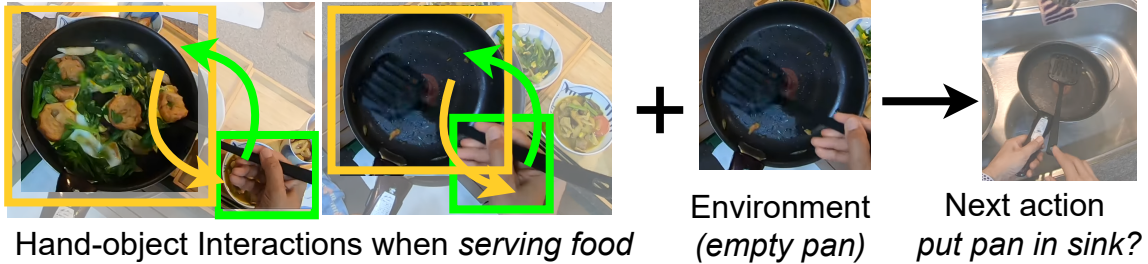


Figure 1: Modeling hand-object interactions and infusing environment to predict the next action. We model the interactions between the hand and the pan while serving food. We infuse the environment context containing the empty pan into the interactions to predict the next action.

compared to when it lies on a table. Our hand also looks different when it holds a spoon compared to a plate. Another motivation to model all the hand-object interactions is some actions are better represented by more than one interaction. In such a case, we need to consider other objects around the hand apart from the object involved in the next action. For example, a knife is crucial to *cut a pizza*. So, both *holding* knife and *pizza* are essential for anticipating *cut pizza*.

Although hand-object interactions are critical for action anticipation, most prior works only focus on the appearance of the entire video [18, 60], motion [45], detected objects [13], or a combination of all of the above [13, 52]. Although [47] presents a model for human-object interactions for action anticipation, it does not exploit the visual changes in humans and objects’ appearance caused by the execution of actions. *We propose a novel way to model human-object interactions that involve computing the change in the appearance of objects and humans due to executing the action.* In fact, specific actions may cause specific changes in the appearance of objects, the environment, and even the appearance of hands. We design a spatio-temporal visual transformer denoted as human-object Interaction visual transformer (InAViT) for action anticipation that refines *interaction tokens* in every frame. The interaction tokens are obtained from refined object and human tokens and the refinement is influenced by objects, hands, and the anticipated action. We incorporate the environment information (contextual cues) into interaction tokens by proposing a trajectory cross-attention mechanism based on trajectory attention [42]. Finally, we infuse interaction tokens into the observed video to build an interaction-centric video representation for effective action anticipation.

Human-object interactions in actions are expressed as relations in spatio-temporal graphs [24, 59, 36, 55, 41]. Our approach is inspired by these interaction representation-based approaches especially the progression of human-object relationships for action recognition tasks [41]. However, our interaction-centric video representation recognizes humans as a separate entity from objects that affect visual change on objects and vice-versa. Object-centric approaches consider only object dynamics [23, 64] and do not treat human hands as a separate entity [36]. However, consecutive egocentric actions may only be connected by hand movement. For example, *washing a dish* followed by *closing tap* are connected only through hand movement. The hand causes a visual change in both these objects and also changes in appearance while interacting with them. Modeling the changes in both hand and objects through hand-object interactions connects these actions better than observing the change in objects alone. Therefore, we postulate that human-object interaction-centric representations are better suited for action anticipation than object-centric approaches. Specifically, we leverage the recent trajectory attention-based MotionFormer model [42] to build the interaction-centric video representation. In summary, our contributions are:

- We propose a novel Transformer-based interaction model that computes appearance change in objects and hands occurring due to execution of action and models these changes in appearances to refine the video representation for action anticipation. To the best of our knowledge, we are the first to demonstrate the efficacy of hand-object interactions for egocentric action anticipation.

- On the EK100 evaluation server, our model InAViT is top the public leaderboard and outperforms the second-best model by 3.3% on mean-top5 recall.

## 2 Related Work

Anticipating human actions has gained interest in the research community with large datasets [20, 38, 9] and innovative approaches [13, 52, 18, 60, 11, 21, 61, 43, 62, 26, 15, 14]. Action anticipation is defined as predicting the next action from the observed action/actions [13]. Before this definition of action anticipation, predicting the future was referred to as early action recognition [50, 57, 51, 46, 15, 58]. Early action recognition refers to predicting the ongoing action using a few frames from the beginning of the action. These approaches predict the visual representation [57] or a low-level representation of the future frames [51, 46]. The first approach that predicts the next future action is [37]. In [37], a linear transition model generates the action label of a frame 1 second into the future. [14] propose a neural memory network that compares the similarity of input and existing memory content to store/discard crucial information for future action prediction. In [13], rolling and unrolling LSTM (RU-LSTM) is proposed to predict the next action. A multi-modal attention module chooses how RGB, optical Flow, and bag-of-objects should be best combined. In [52], RU-LSTM is given more temporal context in the form of non-local blocks that combine local and global temporal context. In [18], spatio-temporal transformers called Anticipative Video Transformers (AVT) are proposed for action anticipation. The temporal transformer combines the patch representation from spatial visual transformers (ViT) across frames to predict a single future feature and action label. In [60], AVT is extended to incorporate long-range sequences by memory caching multiple smaller temporal sequences.

While next action prediction is concerned with the near future, long-term action forecasting involves anticipating multiple future actions and their duration. In [2], both RNNs and CNNs are explored to model the observed actions and duration and predict future actions and their corresponding duration. [1] introduces uncertainty modeling in action forecasting using variational latent distribution learned by the RNN in [2]. [35] uses the dependence of the duration of future actions on labels using a multi-headed variational RNN to predict future actions and duration effectively. In [26] temporal convolutions are proposed with varying time as a parameter to predict future actions for different time horizons. [40] proposes a GRU-based Encoder-Decoder to compare observed and future action distributions via optimal transport loss to predict the best future action. [19] utilizing global self-attention across past and future actions in a Transformer based Encoder-Decoder architecture to predict multiple future actions in parallel. [39] extends [52] using two transformer encoders for short-term (segment-level) and long-term (video-level) encoding and fuses them in a decoder to predict future actions.

Different from the above approaches, [48, 49] focus on modeling a goal representation to predict the next action. Other approaches consider past and future correlation using Jaccard vector similarity [11], self-regulated learning [43], transitional model [37], and counterfactual reasoning [65]. However, none of these approaches consider or model human-object interactions to predict the next action. Only [47] considers human-object interactions by concatenating human and object features but it does not model the visual change in the object or hand because of each other. Also, [47] does not have a mechanism to imbibe environment (video) into interactions like our approach.

There are a variety of approaches for Human-Object Interactions (HOIs) modeling in images [5, 17, 30, 16, 63, 6, 27, 28, 31]. HOI modeling in videos is severely understudied [32, 29, 33, 25]. In [29], human-object interaction regions are detected in videos using verb-object queries describing the action. Observed action labels are not available during testing in action anticipation and hence, we cannot predict the interaction region. In [25], relationships between humans and objects are modeled and verified using relationship labels. Relationship labels are not available for the observed video and so our model attends to all interactions and discovers their importance in predicting the next action.

Another related area is interaction hotspot prediction where future hand-trajectory and interaction spots need to be estimated. Interaction prediction approaches [32, 33] learn future hand motion distribution conditioned on the video representation using an encoder (LSTM [32] or Transformer [33]).

Then, hand trajectories are sampled from the encoder to build an interaction hot-spot distribution using a decoder. However, these approaches require explicit annotations of hand trajectories in future, object trajectories in the observed frames, and distribution of interaction spots in the future. Our interaction modeling approach obviates the need for hand and object trajectory annotations that are difficult to obtain in videos as shown in [12].

### 3 Overview of modeling interaction for action anticipation

This section provides an overview of our interaction modeling method for action anticipation. We describe different interaction modeling methods in Section 4, interaction refinement using environment in Section 5.1, and obtaining interaction-centric video representation for action anticipation in Section 5.2.

We extract a set of 3-D cuboids or video "tokens" from the video as existing video transformers [3, 42, 4]. The set of all the video tokens from a single fixed length video-clip is denoted by  $X \in \mathbb{R}^{THW \times d}$  wherein each of the  $THW$  cuboids is linearly projected to a  $d$ -dimensional vector. Let  $\mathbf{x}_{st} \in \mathbb{R}^d$  denote a video token from the set  $X$  at spatial location  $s \in \{1, \dots, H \times W\}$  and temporal location  $t \in \{1, \dots, T\}$ . Similar to [42], we add separate learnable positional encoding for spatial and temporal dimension for each video token denoted as  $\mathbf{e}_s^s \in \mathbb{R}^d$  and  $\mathbf{e}_t^t \in \mathbb{R}^d$ , respectively. The resultant video token after spatial and temporal embedding is given as  $\mathbf{x}_{st} = \mathbf{x}_{st} + \mathbf{e}_s^s + \mathbf{e}_t^t$ . A classification token  $\mathbf{x}_{cls}$  is appended for anticipating the next action from  $X$  resulting in  $THW + 1$  tokens in  $\mathbb{R}^d$ . We exclude the classification token hereafter for clarity.

In egocentric action anticipation, hands and objects play a key role in anticipating actions. Let us illustrate using an example of serving the contents of a pan using a spatula. Here, the *interaction* between the hand and pan is the changing appearance of the pan from full to half-full to empty, the changing appearance of the spatula when it is used to scoop the food from empty to full to empty, and the change of hand pose while scooping and serving. Hands and objects change the appearance of other objects either by occluding the object or causing visible state changes, such as *knife cutting tomato* or *spatula emptying a pan*. Change in the state of the objects determines the next action i.e. empty pan leads to *put the pan in sink* or tomato slices lead to *put tomato in pan*. We capture these changes or interactions in *interaction tokens* by refining hand and object representations with respect to each other.

The hand and object representations we consider are hand tokens  $\mathcal{H}$  and object tokens  $\mathcal{O}$  extracted from the video tokens (Section 4.1). The refinement of hand tokens uses all the object tokens in the frame (as in Eq. (1)). The refinement for every object token is done using hand tokens and other object tokens in the frame (as in Eq. (2)).

$$\tilde{\mathcal{H}} = \phi_{\mathcal{H}}(\mathcal{H}|\mathcal{O}) \tag{1}$$

$$\tilde{\mathcal{O}}_i = \phi_{\mathcal{O}}(\mathcal{O}_i|\mathcal{H}, \mathcal{O}_j) \quad \forall j \neq i, i \in 1, \dots, N, \tag{2}$$

Here  $\phi_{\mathcal{H}}$  and  $\phi_{\mathcal{O}}$  are cross attention functions (Section 4.2). Refined object tokens for all objects are denoted as  $\tilde{\mathcal{O}} = [\tilde{\mathcal{O}}_1, \dots, \tilde{\mathcal{O}}_N]$ . Together, the refined hand and object tokens constitute the interaction tokens  $I = [\tilde{\mathcal{H}}, \tilde{\mathcal{O}}]$ .

We note that the environment or the background of the current action may provide useful information when predicting the next action. For example, *picking a tomato* next to the cutting board (environment) informs that the next actions are probably *cut tomato*. Therefore, we enrich the interaction tokens ( $I$ ) using the information coming from the environment and vice-versa. We use Trajectory Cross Attention function ( $\phi_I$ ) inspired by [42] to obtain the environment-refined interaction tokens  $\tilde{I}$

$$\tilde{I} = \phi_I(I|X). \tag{3}$$

The final video representation is interaction-centric where we first concatenate environment-refined interaction to the video tokens. Then, we assimilate the interaction information into the video using self-attention ( $\phi_X$ ). We choose the refined tokens corresponding to the original video tokens  $X$  as the

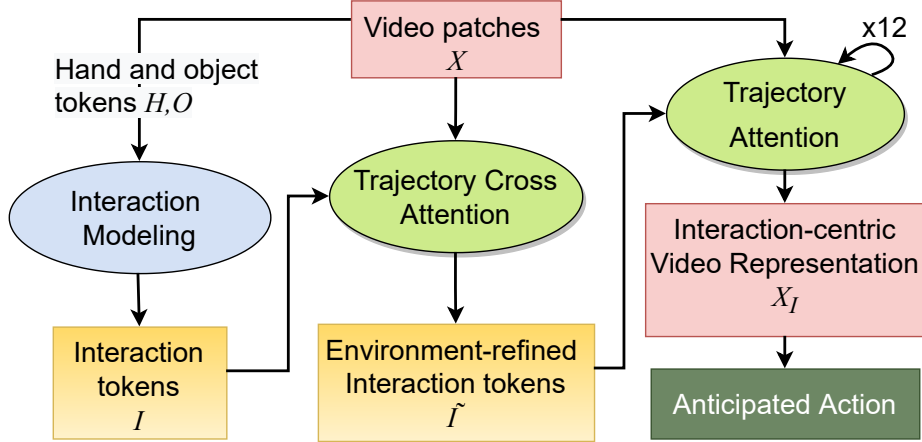


Figure 2: Block diagram of our interaction modeling based action anticipation. Ellipses represent the different processing mechanisms. Trajectory attention  $\times 12$  refers to MotionFormer. Yellow rectangles show interaction tokens and red rectangles show video representations.

interaction-centric video representation  $X_I$

$$X_I = \phi_X([\tilde{I}, X]). \quad (4)$$

We predict the next action using the interaction-centric video representation with multiple layers of Trajectory Attention as in MotionFormer [42]

$$\mathbf{a}_{next} = \phi(X_I). \quad (5)$$

Next action anticipation is defined as observing  $1, \dots, T$  frames and predicting the action that happens after a gap of  $T_a$  seconds. It is important to note that a new action starts after  $T_a$  seconds that is not seen in the observed frames. Our overall approach is shown in Fig. 2.

## 4 Modeling Interaction Tokens

We model spatio-temporal interaction between hands and objects in three ways encapsulating different types of interaction information. First, we use Spatial Cross Attention (SCA) between hands and objects as described in Section 4.3. We compute the change in hand tokens by cross-attention with object tokens and vice-versa. Second, we use Self Attention of hands/object token Over Time (SOT) as described in Section 4.4. We refine hand tokens only using hand tokens from all the frames. Similarly, we refine each object token using the same object token from all the frames. Third, we construct a Union Box (UB) with the hand and the nearest object in every frame as described in Section 4.5. We refine union box tokens to model change which results in the third type of interaction tokens.

Interaction tokens are based on hand and object tokens and we describe how to obtain them in Section 4.1. We also define cross-attention and self-attention operations in Section 4.2 as they will be used in different parts of our model.

### 4.1 Obtaining Hand and Object Tokens

We use the bounding boxes for hands and objects in each frame to obtain hand and object representations from video tokens  $X$ . We obtain the object and hand detections using Faster R-CNN [44]. In every frame, we use one bounding box for the hand and  $N$  bounding boxes for objects closest to the hand. SORT algorithm is used over the detections to obtain sequences of detections where each sequence represents a hand or an object [41].

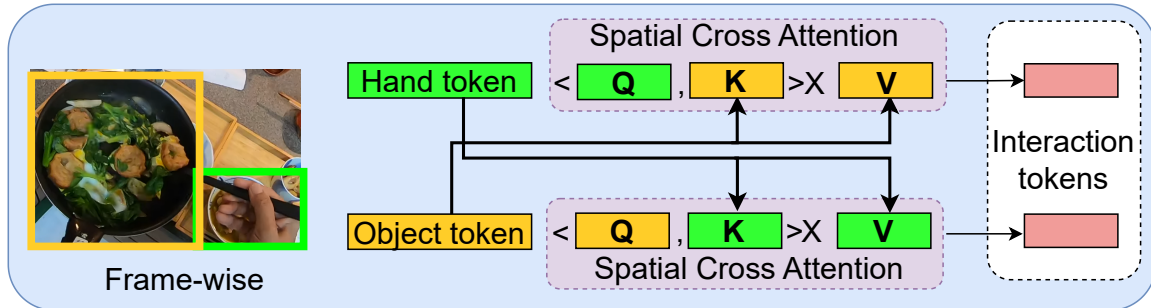


Figure 3: Modeling interaction tokens using Spatial Cross Attention. In every frame, we use the hand tokens as query and object tokens as key and value to compute the refined hand tokens. Refined object tokens are computed with the object token as query and hand token and other object tokens as key and values (not shown here to avoid clutter). Interaction tokens consist of both refined hand and object tokens.

Now, given the video tokens corresponding to a frame  $X_t$  and the bounding box of the hand  $B_{h,t}$ , we aim to obtain a hand token  $\mathbf{h}_t \in \mathbb{R}^d$ . So, we apply RoIAlign [22] layer on  $X_t$  using the bounding box to obtain hand region crops similar to [23]. We then use MLP and max-pooling to obtain the final hand representation or the hand token.

$$\mathbf{h}_t = MLP(MaxPool(RoIAlign(X_t, B_{h,t}))) \quad (6)$$

We apply this to every frame to obtain  $T$  hand tokens denoted by  $\mathcal{H} \in \mathbb{R}^{T \times d}$  where  $\mathcal{H} = [\mathbf{h}_1, \dots, \mathbf{h}_T]$ . Similarly, for each of object  $i$ , we obtain a  $T$  object tokens  $\mathbf{o}_{i,1}, \dots, \mathbf{o}_{i,T}$  and we denote it as  $\mathcal{O}_i \in \mathbb{R}^{T \times d}$ . In total, for the  $N$  objects, we end up with  $\mathcal{O} \in \mathbb{R}^{T \times N \times d}$  where  $\mathcal{O} = [\mathcal{O}_1, \dots, \mathcal{O}_N]$ .

## 4.2 Cross-Attention and Self-Attention

In cross-attention, queries are obtained from the target that needs to be refined. The key and values are obtained from the source that needs to be queried to obtain the refined target tokens. Let  $\mathbf{a}_m \in A$  be a target token from all target tokens  $A$  and  $\mathbf{b}_n \in B$  be a source token from all the source tokens  $B$ . The queries, keys, and values are constructed as

$$\mathbf{q} = \mathbf{a}_m \mathbf{W}_q, \mathbf{k} = \mathbf{b}_n \mathbf{W}_k, \mathbf{v} = \mathbf{b}_n \mathbf{W}_v \quad (7)$$

where  $\mathbf{W}_q, \mathbf{W}_k, \mathbf{W}_v$  are learnable weights. In the rest of the paper, we use  $\mathbf{W}_q, \mathbf{W}_k$ , and  $\mathbf{W}_v$ , as learnable weights query, key, and value, respectively, for all attention operations. We do this for clarity in notation but all the weights are different and learned independently. In self-attention, query, key, and value are all obtained from target tokens  $\mathbf{a}_m \in A$ .

$$\mathbf{q} = \mathbf{a}_m \mathbf{W}_q, \mathbf{k} = \mathbf{a}_m \mathbf{W}_k, \mathbf{v} = \mathbf{a}_m \mathbf{W}_v \quad (8)$$

The output of both cross-attention and self-attention is the refined target token  $\tilde{\mathbf{a}}_m$ .

$$\tilde{\mathbf{a}}_m = \sum \mathbf{v} \frac{\exp \langle \mathbf{q}, \mathbf{k} \rangle}{\sum \exp \langle \mathbf{q}, \mathbf{k} \rangle} \quad (9)$$

We omit the factor  $d^{1/2}$  for clarity and assume that both queries and keys have been scaled by  $d^{1/4}$  [56].

## 4.3 SCA - Spatial Cross-Attention between hands and objects

In every observed frame, there is a hand token and multiple object tokens. We model the change in hands by cross-attention as shown in Fig. 3. We use the hand token  $\mathbf{h}_t$  as the query and compute

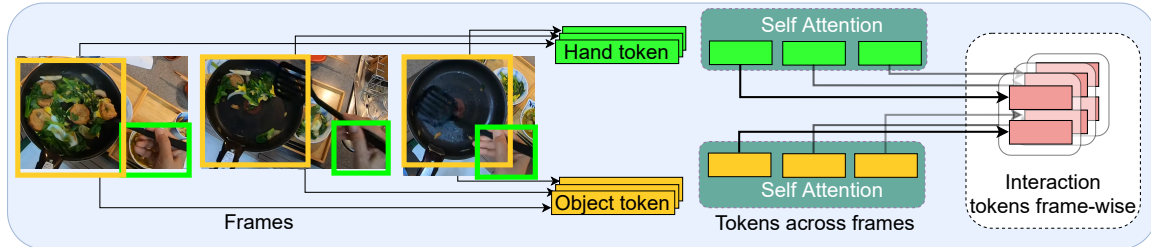


Figure 4: Modeling interaction tokens using Self-attention Over Time. We compute self-attention over hand tokens in all the frames to obtain refined hand tokens. We repeat this for every object region across frames. The refined hand and object tokens at every frame are the interaction tokens for that frame.

the attention with respect to every object token in the same frame  $\mathbf{o}_{1,t}, \dots, \mathbf{o}_{N,t}$ . The query, key, and value are denoted as  $\mathbf{q}_{h,t} = \mathbf{h}_t \mathbf{W}_q$ ,  $\mathbf{k}_{i,t} = \mathbf{o}_{i,t} \mathbf{W}_k$ , and  $\mathbf{v}_{i,t} = \mathbf{o}_{i,t} \mathbf{W}_v$ , respectively. We use cross-attention (Eq. (9)) to get the refined the hand tokens,  $\tilde{\mathbf{h}}_t$ . Cross attention implicitly seeks the object token that the most impact on the hand token by pooling all the object tokens in the frame and weighing each by its probability.

Similarly, we use cross-attention to refine each object token using the hand token and other object tokens in the frame. Every object token  $\mathbf{o}_{i,t}$  acts as a query, and human and other object tokens act as keys and values. Let  $\mathbf{z}_t$  represent either hand or other object tokens in the frame  $t$ . There are  $N$  such tokens in each frame for each object query  $\mathbf{o}_{i,t}$ . The query, key, and values are obtained as  $\mathbf{q}_{i,t} = \mathbf{o}_{i,t} \mathbf{W}_q$ ,  $\mathbf{k}_{j,t} = \mathbf{z}_t \mathbf{W}_k$ , and  $\mathbf{v}_{j,t} = \mathbf{z}_t \mathbf{W}_v$ , respectively. The refined object token  $\tilde{\mathbf{o}}_{i,t}$  are obtained using cross-attention (Eq. (9)).

We call the refined hand and object tokens as interaction tokens  $I_t = [\tilde{\mathbf{h}}_t, \tilde{\mathbf{o}}_{1,t}, \dots, \tilde{\mathbf{o}}_{N,t}]$ . We perform spatial cross-attention over every frame to obtain all the interaction tokens  $I \in \mathbb{R}^{T \times (N+1) \times d}$  and we call this method **SCA** for short. It should be noted that our interaction tokens are different from graph-based interaction modeling [41] where the interaction between humans and objects is captured in the edges but not within each hand and object explicitly as change/refinement.

#### 4.4 SOT - Self-attention of hand/object Over Time

Next, we model interaction tokens as the change in hands and objects individually over time as shown in Fig. 4. Hand token  $h_t$  is refined using only other hand tokens. The query, key, and value all come from the hand tokens across all frames  $\mathbf{q}_{h,t} = \mathbf{h}_t \mathbf{W}_q$ ,  $\mathbf{k}_{h,t} = \mathbf{h}_t \mathbf{W}_k$ ,  $\mathbf{v}_{h,t} = \mathbf{h}_t \mathbf{W}_v$ . Using self-attention (Eq. (9)), we obtain the refined hand tokens  $\tilde{\mathbf{h}}_t$ . We similarly refine object tokens  $\mathbf{o}_{i,t}$  of every object  $i$  separately. The query, key, and value for object  $i$  are computed from its own tokens over all the frames  $\mathbf{q}_{i,t} = \mathbf{o}_{i,t} \mathbf{W}_q$ ,  $\mathbf{k}_{i,t} = \mathbf{o}_{i,t} \mathbf{W}_k$ ,  $\mathbf{v}_t = \mathbf{o}_{i,t} \mathbf{W}_v$ . We obtain refined object tokens  $\tilde{\mathbf{o}}_{i,t}$  using self-attention (Eq. (9)). We call this method Self-attention Over time **SOT** and SOT interaction tokens  $I_t = [\tilde{\mathbf{h}}_t, \tilde{\mathbf{o}}_{1,t}, \dots, \tilde{\mathbf{o}}_{N,t}]$  consist of refined hand and object tokens.

#### 4.5 UB - Union Box of hand and nearest object

Next, we obtain the third type of interaction tokens using the hand and the nearest object to it in every frame as shown in Fig. 5. We compute the union bounding box from the hand and the nearest object bounding boxes in every frame. Here the hand and object union box is similar to the union of objects and human regions for interaction detection [29]. We then get union tokens  $\mathcal{U} \in \mathbb{R}^{T \times d}$  similar to hand and object tokens described in Section 4.1. Unlike the previous two approaches, we refine the human and objects together as part of the union token  $\tilde{\mathbf{u}}_t \in \mathcal{U}$  using self-attention (Eq. (9)) to obtain  $\tilde{\mathbf{u}}_t$ . We call this approach **UB** and the refined union token is the interaction token for the frame  $I_t = \tilde{\mathbf{u}}_t$  where  $I_t \in \mathbb{R}^{T \times d}$ .



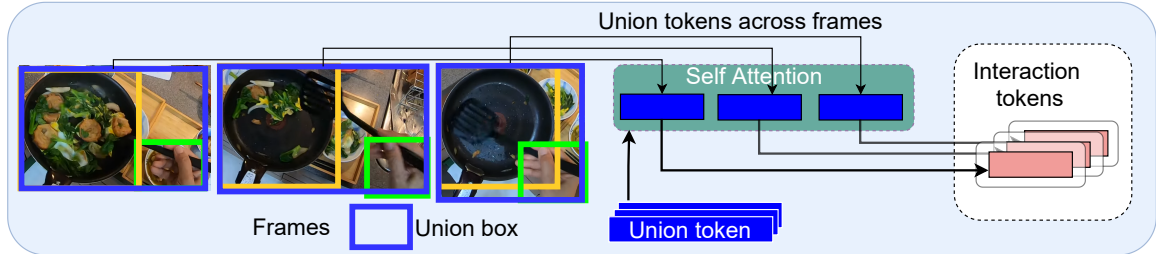


Figure 5: Modeling interaction using Union Boxes. We compute the union bounding box of the hand with the nearest object in every frame. We then compute self-attention to refine the union tokens which are our interaction tokens.

## 5 Interaction Refinement with Environment

In this section, we first describe the process for obtaining environment-refined interaction tokens in Section 5.1. Then, in Section 5.2, we describe how refined interactions are used to obtain interaction-centric video representation for action anticipation.

### 5.1 Environment-refined interaction tokens

The environment plays an important role along with interaction in deciding what are the possible next actions. For example, *washing a plate* with *kitchen sink* as the environment suggests that the next action is probably *close the tap* or *wash other plate/utensils*. So, we incorporate the environment into interaction tokens by proposing Trajectory Cross Attention (TCA) based on trajectory attention [42]. TCA maintains temporal correspondences between the interaction tokens with the relevant environment tokens in the frame as shown in Fig. 6.

Our TCA formulation seeks the probabilistic path of an interaction token between frames. The interaction tokens act as the query on the video tokens  $X$  that is representative of the environment. Let the video patch at spatial location  $s$  in frame  $t$  be given by  $\mathbf{x}_{st} \in \mathbb{R}^d$ . The key and value are obtained from the video patch. We have  $N + 1$  interaction tokens<sup>1</sup> in every frame. For each interaction token  $\mathbf{y}_t \in I_t$ , we obtain a set of trajectory tokens  $\hat{\mathbf{y}}_{tt'} \in \mathbb{R}^d, \forall t' \geq t$  that represents pooled information weighted by the trajectory probability. The pooling operation implicitly looks for the best location  $s$  at frame  $t' \geq t$  by comparing the interaction query  $\mathbf{q}_t = \mathbf{y}_t \mathbf{W}_q$  to the environment keys  $\mathbf{k}_{st'} = \mathbf{x}_{st'} \mathbf{W}_k$  using Eq. (9). The attention is applied spatially and independently for all the interaction tokens in every frame. This is complementary to our previously computed cross attention (Eq. (1) and Eq. (2)) where connections are explored between foreground hand and object tokens. In TCA, we seek connections between refined hand/object (interaction) tokens and the environment.

Once trajectories are computed, we pool them across time to reason about connections across the interaction regions in a frame given the environment. For temporal pooling, the trajectory tokens are projected to a new set of queries, keys, and values  $\hat{\mathbf{q}}_{tt'} = \hat{\mathbf{y}}_{tt'} \mathbf{W}_q$ ,  $\hat{\mathbf{k}}_{tt'} = \hat{\mathbf{y}}_{tt'} \mathbf{W}_k$ ,  $\hat{\mathbf{v}}_{tt'} = \hat{\mathbf{y}}_{tt'} \mathbf{W}_v$ , respectively. The new query  $\hat{\mathbf{q}}_{tt'}$  has information across the entire trajectory that extends across the entire observed video frames. We perform temporal pooling using 1D attention across the new time (trajectory) dimension to obtain the environment-refined interaction tokens (Eq. (9)). We term these refined tokens as *environment-refined interaction tokens*  $\tilde{I} = [\tilde{\mathbf{y}}_1, \dots, \tilde{\mathbf{y}}_T]$ .

### 5.2 Interaction-centric video representation

The next action is dependent on interactions and environment as we discussed in Section 5. So, our goal is to obtain a video representation that incorporates the information from the environment-refined interaction tokens. First, we concatenate the original video tokens  $X$  and the environment-refined

<sup>1</sup>in case of UB interaction modeling



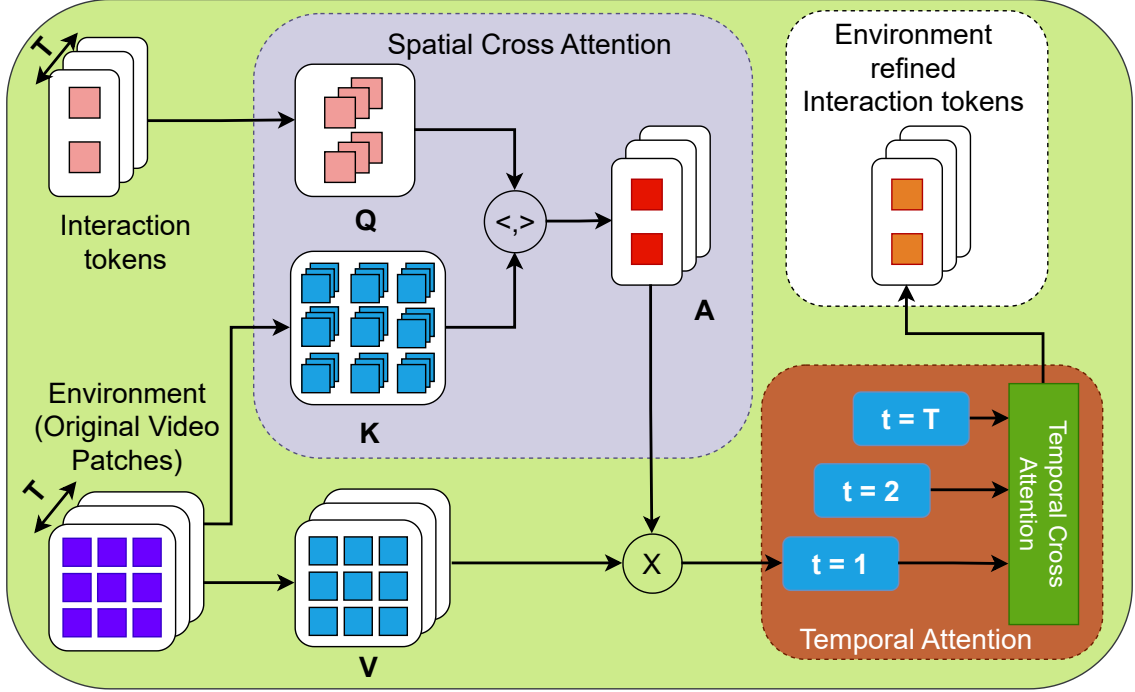


Figure 6: Interaction region refinement with environment using Trajectory Cross Attention. We compute spatial cross-attention (SCA) to find the best location for interaction trajectory by comparing the interaction query to the environment keys. Next, we pool the interaction trajectories across time to form connections across the interaction tokens in a frame given the environment.

interaction tokens  $\tilde{I}$  to form the augmented video representation  $X_a$ <sup>2</sup>. Then we perform self-attention (Eq. (9)) over all the augmented video tokens  $\mathbf{x}_r^a \in X_a$  wherein video tokens attend over the interaction tokens and vice-versa. After self-attention, we obtain refined augmented video tokens  $\tilde{\mathbf{x}}_r^a$ . We construct the interaction-centric video representation  $X_I$  using  $\tilde{\mathbf{x}}_r^a$  that corresponds to the original video tokens.

$$X_I = \tilde{\mathbf{x}}_r^a, \forall r, \text{ if } \mathbf{x}_r^a \in X. \quad (10)$$

We call  $X_I$  as interaction-centric video representation in the same vein as object-centric video representation [23].

Till now, we have only applied a single attention layer for interaction modeling, interaction refinement using environment, and interaction-centric video representation. In literature, video transformer approaches [42, 41, 3] have shown excellent performance with multiple layers of attention. We apply 12 layers of Trajectory Attention following MotionFormer [42] on the interaction-centric video representation to obtain the final video representation  $\tilde{X}_I$ . The reason for choosing MotionFormer is that it performs best empirically. The classification token  $\mathbf{x}_{cls}$  obtained at the end of multiple trajectory attention layers is used to predict the next action, i.e.,  $\hat{\mathbf{a}}_{next} = \phi(\tilde{\mathbf{x}}_{cls})$  where  $\phi$  is a linear layer.

**Loss function.** We use cross-entropy loss for the next action label to train our model. We compare the model’s prediction  $\hat{\mathbf{a}}_{next}$  with the ground truth one-hot label  $\mathbf{a}_{next}$  for the next action as follows

$$\mathcal{L}_{ant} = - \sum \mathbf{a}_{next} \odot \log(\hat{\mathbf{a}}_{next}). \quad (11)$$

It should be noted that as we train our model with the cross-entropy loss to predict the next action,

<sup>2</sup> $X_a \in \mathbb{R}^{T \times (H \times W + N + 1) \times d}$  (for SCA and SOT) or  $X_a \in \mathbb{R}^{T \times (H \times W + 1) \times d}$  for UB

the interaction tokens are optimized for finding the most influential interactions when predicting the next action. Visualization of this is shown in Fig. 7.

## 6 Experiments and Results

### 6.1 Datasets and Implementation Details

We evaluate and compare our methods on two large unscripted action anticipation datasets *EPIC-KITCHENS100*[9] (EK100) and *EGTEA Gaze+*[38]. For EK100, we report results on the test set evaluation server that uses mean-top5 recall as the metric. For EK100 and EGTEA, anticipation gap ( $T_a$ ) is 1s and 0.5s, respectively.

We follow MotionFormer [42] and use 16-frame long clips of resolution  $224 \times 224$  uniformly sampled from an observed video of 64 frames (approximately 2s). Every 3D video token is extracted from a video patch of size  $2 \times 16 \times 16$ . We extract hand, object, and union tokens following the strategy explained in Section 4.1. Then, to implement InAViT(SCA) (Section 4.3), we use a single cross-attention layer with 12 attention heads. Similarly, InAViT(SOT) and InAViT(UB) are implemented with self-attention layer with 12 heads. We set the number of objects per frame as 4 for EK100 and 2 for EGTEA based on empirical performance (this also makes sure batch processing is efficient). We report the results of varying the number of objects per frame in Supplementary. If there are fewer objects (less than 4 or 2 respectively), then we zero pad them and generate null tokens which will not impact the model. The same configuration of objects is used for training other baseline models such as ORViT-MF [23]. The number of hand regions per-frame is set to  $1^3$  as both hands are not visible in most of the instances. If there are two hands in the frame, we randomly pick one and track it using SORT.

We use one layer of trajectory cross-attention with 12 attention heads and a temporal resolution of 8 to obtain the environment refinement of interaction tokens (Section 5.1). We then concatenate the refined interaction and original video tokens to form the augmented video tokens. We use a single self-attention layer with 12 heads on the augmented video tokens to obtain interaction-centric video tokens (Section 5.2). Finally, we apply MotionFormer on the interaction-centric video tokens to predict the next action (Section 5.2). We use a batch size of 16 video(clips) to train on 4 RTX A5000 GPUs with 24 GB memory each and the learning rate is set to  $1e^{-4}$  with AdamW optimizer. We will release our code.

### 6.2 Ablation on InAViT

**Component-wise validation.** In Tab. 1(a), we show the contribution of each component of InAViT - interaction modeling using SCA, environment refinement of interaction tokens (TCA), and interaction-centric video representation using Trajectory Attention (TA) [42]. Environment refinement (SCA+TCA) improves overall performance but we see the biggest improvement when we add TA. So, we conclude that interactions and the video contain complementary information for anticipation.

**Comparing Interaction Modeling.** In Tab. 1(b), we compare the three models for interaction modeling - spatial cross attention (SCA+TCA+TA), spatial attention over time (SOT+TCA+TA), and union boxes (UB+TCA+TA) described in Section 4. In our comparison, SCA performs the best on overall, unseen, and tail classes compared to both SOT and UB. SCA contextualizes the visual change of each hand/object better using other objects compared to SOT which computes visual change individually. UB’s focus is narrower than SCA as it only considers the nearest object that potentially leaves out other close objects which can be used in the next action. SCA performs much better in tail classes where few examples are available and the model relies on visual information for anticipation. As SCA uses all the objects to model interactions, it extracts the most visual information from every frame to make better predictions.

---

<sup>3</sup>All observed actions in EK100 and EGTEA were found to have at least one hand visible during the observation period.

Method	Overall Action(%)	Unseen Action(%)	Tail Action(%)
SCA	12.66	15.49	06.03
SCA + TCA	14.21	14.26	09.12
SCA+TA	22.21	20.85	17.07
SCA + TCA + TA	<b>23.75</b>	<b>23.49</b>	<b>18.11</b>
(a) Component-wise validation of InAViT			
UB+TCA+TA	22.75	22.14	17.04
SOT+TCA+TA	22.48	20.56	17.46
(b) Comparing interaction modeling methods			
SCA-(Hand)+TCA+TA	23.27	23.21	17.57
SCA-(Obj)+TCA+TA	22.49	22.23	16.73
(c) Comparing refined hand vs. object as interaction tokens			
SCA+TCA(Mask FG)+TA	08.05	05.92	05.84
SCA+Env.Ref(Concat)+TA	22.14	23.47	17.24
(d) Effect of environment			

Table 1: Ablation of InaViT on EK100 evaluation server. TCA=Environment refinement using TCA, TA=Trajectory Attention for interaction video representation, Mask FG=Masked foreground in environment, Env.Ref(Concat)=Environment refinement with concatenation, not TCA. Verb and Noun results are in Supplementary.

**Comparing refined Hand vs. Object tokens.** The best-performing SCA interaction model involves the refinement of hand and object tokens to obtain interaction tokens. In Tab. 1(c), we compare the contribution of refined hand (SCA(Hand)+TCA+TA) and object tokens (SCA(Obj)+TCA+TA) by using them independently as interaction tokens. As in SCA formulation, we refine hand tokens with objects and object tokens with hand and other objects. Refined hand tokens perform better than refined object tokens as the position of the hand is vital in determining what object(s) can be used next. Still, interaction tokens containing both refined hands and object tokens (SCA+TCA+TA) performs the best. We conclude that modeling the changes in hand and object tokens provide complementary information to improve action anticipation.

**Effect of environment refinement.** We evaluate the effect of environment refinement on interaction tokens in Tab. 1(d). For this comparison, we change either the input or mechanism of environment refinement(Section 5.1). Interaction modeling is done using SCA and interaction-centric video representation is computed using the original video tokens. At first, we remove the foreground i.e. hands and objects from the environment. We crop the objects and hands based on the bounding boxes and apply a Gaussian filter to soften the edges. We call this masked foreground environment and use it to refine interaction tokens. The performance of (SCA+TCA(Mask FG)+TA) is quite poor which means that the complete environment with foreground objects (SCA+TCA+TA) is better for refinement. We also find that the concatenation of environment (video tokens) to interaction tokens (SCA+Env.Ref(Concat)+TA) is worse than our proposed Trajectory Cross-attention for environment refinement (SCA+TCA+TA).

### 6.3 Comparison with state-of-the-art

We now compare our best-performing InAViT (SCA+TCA+TA) model against state-of-the-art approaches. On EK100 evaluation server, InAViT significantly outperforms other approaches as seen

Method	Overall (%)			Unseen (%)			Tail (%)		
	Verb	Noun	Action	Verb	Noun	Action	Verb	Noun	Action
AFFT [66]	20.70	31.80	14.90	16.20	27.70	12.10	13.40	23.80	11.80
AVT [18]	26.69	32.33	16.74	21.03	27.64	12.89	19.28	24.03	13.81
Abs. goal [49]	31.40	30.10	14.29	31.36	35.56	17.34	22.90	16.42	07.70
TransAction [21]	36.15	32.20	13.39	27.60	24.24	10.05	32.06	29.87	11.88
MF*	45.14	45.97	19.75	40.36	45.28	19.49	39.17	35.91	14.11
ORViT-MF*	43.74	46.61	21.53	38.99	45.32	21.47	37.28	35.78	15.96
InAViT (Ours)	<b>49.14</b>	<b>49.97</b>	<b>23.75</b>	<b>44.36</b>	<b>49.28</b>	<b>23.49</b>	<b>43.17</b>	<b>39.91</b>	<b>18.11</b>

Table 2: Comparison with state-of-the-art on EK100 evaluation server. \*We trained MF and ORViT-MF for action anticipation using their official repositories. Full table in Supplementary.

Method	Top-1 Accuracy (%)			Mean Class Accuracy (%)		
	VERB	NOUN	ACT.	VERB	NOUN	ACT.
FHOI [32]	49.0	45.5	36.6	32.5	32.7	25.3
AFFT [66]	53.4	50.4	42.5	42.4	44.5	35.2
AVT [18]	54.9	52.2	43.0	49.9	48.3	35.2
Abs. Goal [49]	64.8	65.3	49.8	63.4	55.6	37.4
MF*	77.8	75.6	66.6	77.5	72.1	56.9
ORVIT-MF*	78.8	76.3	67.3	78.8	75.8	57.2
InAViT (Ours)	<b>79.3</b>	<b>77.6</b>	<b>67.8</b>	<b>79.2</b>	<b>76.9</b>	<b>58.2</b>

Table 3: Comparison of anticipation performance on EGTEA Gaze+. Full table in Supplementary.

in Tab. 2. InAViT’s performance is much better than AVT [18] on EK100 which also uses visual transformers for representing the video. We also compare InAViT against the baseline MotionFormer (MF) [42] and object-centric video representation ORViT-MF [23]. As ORViT and MF are not trained for action anticipation, we train them using the official repositories.

We are the first to show the effectiveness of MF and ORVIT-MF for action anticipation which alone outperforms prior state-of-the-art methods. Our approach InAViT performs even better than both MF and ORVIT-MF and achieves significantly better results than previous best results, the Abstract Goal [49] on EGTEA (Tab. 3) and AVT [18] on EK100. In fact, InAViT outperforms [49] by 18% in mean accuracy and 20.8% in top-1 accuracy on EGTEA. It also outperforms human-object interaction method in [32] by 30% and 35% on mean and top-1 accuracy, respectively. Similarly, InAViT outperforms AVT [18] by 22%, 17%, and 7%, in the overall verb, noun, and action anticipation on EK100 which is impressive given the large number of actions (3805), nouns (300), and verbs (97). On EK100, InAViT outperforms AVT on unseen and tail action anticipation by 12% and 4%, respectively. This demonstrates that InAViT is effective at predicting rare actions and generalizes much better to new environments.

In Tab. 4, we vary the anticipation gap ( $T_a$ ) for EGTEA dataset. InAViT’s is more robust for longer anticipation because it can make use of additional human-object interaction information than ORVIT-MF. We also analyzed the computational cost of InAViT and found that the baseline MotionFormer requires 370 GFlops, while InAViT requires 391 GFlops and ORVIT-MF requires 403 GFlops. So, InAViT is less computationally expensive than ORVIT-MF and it performs better on action anticipation.

Top-1 Action Accuracy	Anticipation gap ( $T_a$ in s)			
	2	1.5	1	0.5
MF*	60.2	61.7	64.2	66.6
ORViT-MF*	62.2	63.6	66.1	67.3
InAViT (Ours)	<b>64.1</b>	<b>65.8</b>	<b>66.9</b>	<b>67.8</b>

Table 4: Varying anticipation gap ( $T_a$ ) on EGTEA

## 6.4 Qualitative Results

In Fig. 7, we visualize the attention map of the  $\mathbf{x}_{cls}$  token used for action anticipation on all spatial tokens across the frames. This helps us understand where InAViT focuses compared to MotionFormer. Motionformer attention is divided into many areas while InAViT attends to the interaction. While anticipating *peel onion* (Fig. 7(a)), InAViT pays high attention to the exact location the onion is being peeled. Similarly, when anticipating *pour sugar* (Fig. 7(b)), InAViT attends to both the cup and the sugar container. The frames for visualization are chosen based on the significant motion of hands and objects during the observed action. We show more qualitative results in Supplementary.

## 7 Discussions and Conclusion

We present a novel hand-object interaction modeling visual transformer InAViT for egocentric action anticipation. We show that refinement of hand and object boxes with respect to each other i.e. SCA is a stronger prior for interaction modeling than isolated refinement as in SOT (Self-attention of hand/object Over Time). We also find that union box comprising of both hands and objects is ineffective at interaction modeling compared to mutual refinement of individual hand and object boxes. We show that incorporating environment information makes interactions more effective at action anticipation. Particularly, using Trajectory Cross Attention for environment-refinement of interaction tokens is better than concatenation. Finally, we show that interaction-centric video representation is better at anticipation than object-centric video representation.

## Acknowledgment

This research/project is supported in part by the National Research Foundation, Singapore under its AI Singapore Program (AISG Award Number: AISG-RP-2019-010) and by the National Research Foundation Singapore and DSO National Laboratories under the AI Singapore Programme (AISG Award No: AISG2-RP-2020-016).

## References

- [1] Yazan Abu Farha and Juergen Gall. Uncertainty-aware anticipation of activities. In *Proceedings of the IEEE/CVF International Conference on Computer Vision Workshops*, pages 0–0, 2019.
- [2] Yazan Abu Farha, Alexander Richard, and Juergen Gall. When will you do what?-anticipating temporal occurrences of activities. In *Proceedings of the IEEE Conference on Computer Vision and Pattern Recognition*, pages 5343–5352, 2018.
- [3] Anurag Arnab, Mostafa Dehghani, Georg Heigold, Chen Sun, Mario Lučić, and Cordelia Schmid. Vivit: A video vision transformer. In *Proceedings of the IEEE/CVF International Conference on Computer Vision*, pages 6836–6846, 2021.
- [4] Gedas Bertasius, Heng Wang, and Lorenzo Torresani. Is space-time attention all you need for video understanding? In *International Conference on Machine Learning*, pages 813–824. PMLR, 2021.

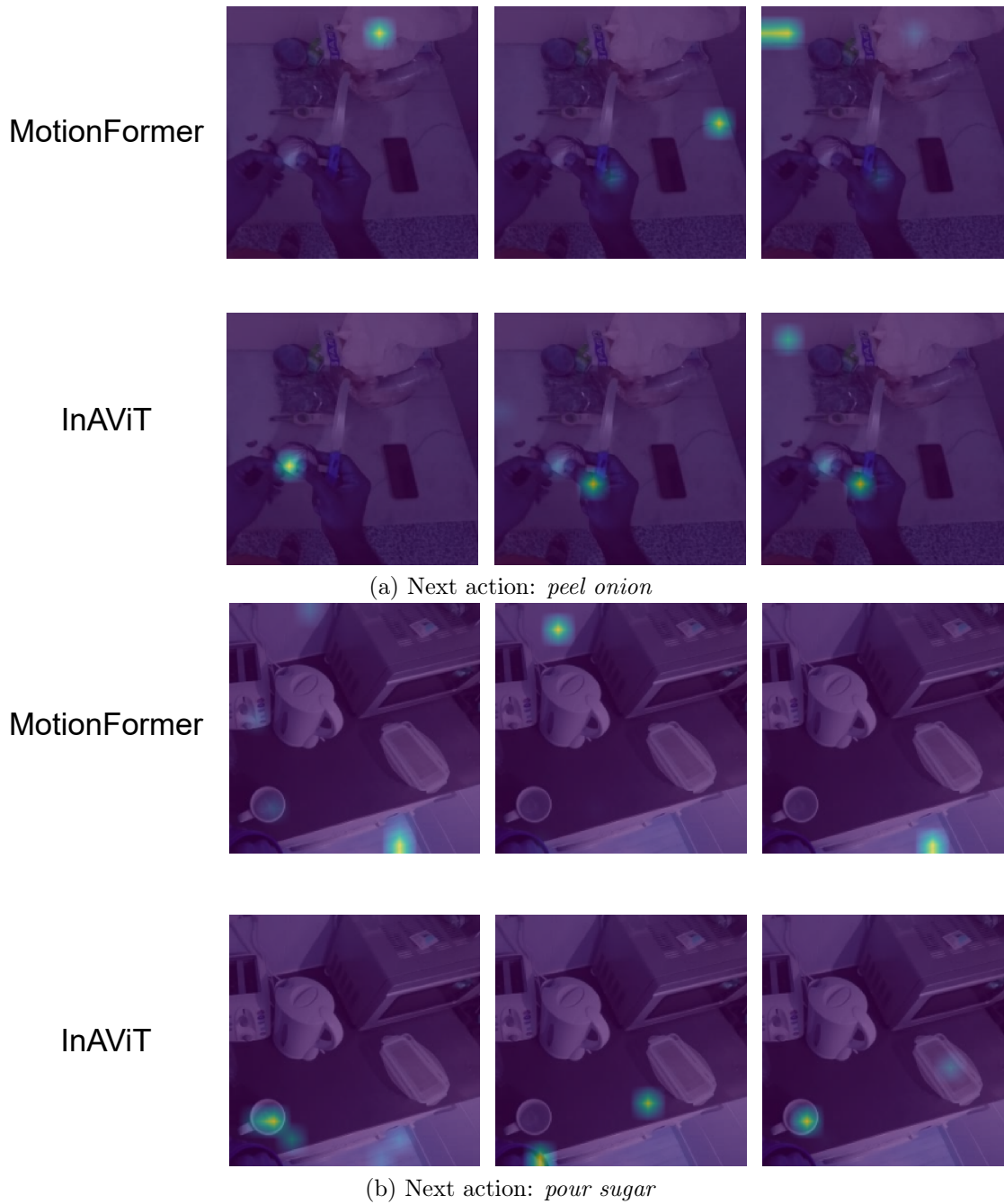


Figure 7: (a) InAViT attends to the location where the onion is being peeled, (b) InAViT attends to both the cup and the sugar container. Examples from EK100.

- [5] Yu-Wei Chao, Yunfan Liu, Xieyang Liu, Huayi Zeng, and Jia Deng. Learning to detect human-object interactions. In *2018 IEEE Winter Conference on Applications of Computer Vision (WACV)*, pages 381–389. IEEE, 2018.
- [6] Mingfei Chen, Yue Liao, Si Liu, Zhiyuan Chen, Fei Wang, and Chen Qian. Reformulating hoi detection as adaptive set prediction. In *Proceedings of the IEEE/CVF Conference on Computer Vision and Pattern Recognition*, pages 9004–9013, 2021.
- [7] Shuyang Chen, Yuan-Chi Peng, John Wason, Jinda Cui, Glenn Saunders, Shridhar Nath, and John T Wen. Software framework for robot-assisted large structure assembly. In *International Manufacturing Science and Engineering Conference*, volume 51371, page V003T02A047. American Society of Mechanical Engineers, 2018.
- [8] Yi Cheng, Fen Fang, and Ying Sun. Team vi-i2r technical report on epic-kitchens-100 unsupervised domain adaptation challenge for action recognition 2021. *arXiv preprint arXiv:2206.02573*, 2022.
- [9] Dima Damen, Hazel Doughty, Giovanni Maria Farinella, Antonino Furnari, Evangelos Kazakos, Jian Ma, Davide Moltisanti, Jonathan Munro, Toby Perrett, Will Price, et al. Rescaling egocentric vision: collection, pipeline and challenges for epic-kitchens-100. *International Journal of Computer Vision*, 130(1):33–55, 2022.
- [10] Eadom Dessalene, Michael Maynard, Chinmaya Devaraj, Cornelia Fermuller, and Yiannis Aloimonos. Egocentric object manipulation graphs. *arXiv preprint arXiv:2006.03201*, 2020.
- [11] Basura Fernando and Samitha Herath. Anticipating human actions by correlating past with the future with jaccard similarity measures. In *Proceedings of the IEEE/CVF Conference on Computer Vision and Pattern Recognition*, pages 13224–13233, 2021.
- [12] David F Fouhey, Wei-cheng Kuo, Alexei A Efros, and Jitendra Malik. From lifestyle vlogs to everyday interactions. In *Proceedings of the IEEE Conference on Computer Vision and Pattern Recognition*, pages 4991–5000, 2018.
- [13] Antonino Furnari and Giovanni Maria Farinella. Rolling-unrolling lstms for action anticipation from first-person video. *IEEE transactions on pattern analysis and machine intelligence*, 43(11):4021–4036, 2020.
- [14] Harshala Gammulle, Simon Denman, Sridha Sridharan, and Clinton Fookes. Forecasting future action sequences with neural memory networks. In *30th British Machine Vision Conference 2019, BMVC 2019, Cardiff, UK, September 9-12, 2019*, page 298. BMVA Press, 2019.
- [15] Harshala Gammulle, Simon Denman, Sridha Sridharan, and Clinton Fookes. Predicting the future: A jointly learnt model for action anticipation. In *Proceedings of the IEEE/CVF International Conference on Computer Vision*, pages 5562–5571, 2019.
- [16] Chen Gao, Jiarui Xu, Yuliang Zou, and Jia-Bin Huang. Drg: Dual relation graph for human-object interaction detection. In *European Conference on Computer Vision*, pages 696–712. Springer, 2020.
- [17] Chen Gao, Yuliang Zou, and Jia-Bin Huang. ican: Instance-centric attention network for human-object interaction detection. *arXiv preprint arXiv:1808.10437*, 2018.
- [18] Rohit Girdhar and Kristen Grauman. Anticipative video transformer. In *Proceedings of the IEEE/CVF International Conference on Computer Vision*, pages 13505–13515, 2021.
- [19] Dayoung Gong, Joonseok Lee, Manjin Kim, Seong Jong Ha, and Minsu Cho. Future transformer for long-term action anticipation. In *Proceedings of the IEEE/CVF Conference on Computer Vision and Pattern Recognition*, pages 3052–3061, 2022.
- [20] Kristen Grauman, Andrew Westbury, Eugene Byrne, Zachary Chavis, Antonino Furnari, Rohit Girdhar, Jackson Hamburger, Hao Jiang, Miao Liu, Xingyu Liu, et al. Ego4d: Around the world in 3,000 hours of egocentric video. In *Proceedings of the IEEE/CVF Conference on Computer Vision and Pattern Recognition*, pages 18995–19012, 2022.
- [21] Xiao Gu, Jianing Qiu, Yao Guo, Benny Lo, and Guang-Zhong Yang. Transaction: ICL-SJTU submission to epic-kitchens action anticipation challenge 2021. *CoRR*, abs/2107.13259, 2021.
- [22] Kaiming He, Georgia Gkioxari, Piotr Dollár, and Ross Girshick. Mask r-cnn. In *Proceedings of the IEEE international conference on computer vision*, pages 2961–2969, 2017.
- [23] Roei Herzig, Elad Ben-Avraham, Karttikeya Mangalam, Amir Bar, Gal Chechik, Anna Rohrbach, Trevor Darrell, and Amir Globerson. Object-region video transformers. In *Proceedings of the IEEE/CVF Conference on Computer Vision and Pattern Recognition*, pages 3148–3159, 2022.
- [24] Ashesh Jain, Amir R Zamir, Silvio Savarese, and Ashutosh Saxena. Structural-rnn: Deep learning on spatio-temporal graphs. In *Proceedings of the IEEE conference on computer vision and pattern recognition*, pages 5308–5317, 2016.
- [25] Jingwei Ji, Rishi Desai, and Juan Carlos Niebles. Detecting human-object relationships in videos. In *Proceedings of the IEEE/CVF International Conference on Computer Vision*, pages 8106–8116, 2021.



- [26] Qihong Ke, Mario Fritz, and Bernt Schiele. Time-conditioned action anticipation in one shot. In *Proceedings of the IEEE/CVF Conference on Computer Vision and Pattern Recognition*, pages 9925–9934, 2019.
- [27] Bumsoo Kim, Taeho Choi, Jaewoo Kang, and Hyunwoo J Kim. Uniondet: Union-level detector towards real-time human-object interaction detection. In *European Conference on Computer Vision*, pages 498–514. Springer, 2020.
- [28] Bumsoo Kim, Junhyun Lee, Jaewoo Kang, Eun-Sol Kim, and Hyunwoo J Kim. Hotr: End-to-end human-object interaction detection with transformers. In *Proceedings of the IEEE/CVF Conference on Computer Vision and Pattern Recognition*, pages 74–83, 2021.
- [29] Shuang Li, Yilun Du, Antonio Torralba, Josef Sivic, and Bryan Russell. Weakly supervised human-object interaction detection in video via contrastive spatiotemporal regions. In *Proceedings of the IEEE/CVF International Conference on Computer Vision*, pages 1845–1855, 2021.
- [30] Yong-Lu Li, Siyuan Zhou, Xijie Huang, Liang Xu, Ze Ma, Hao-Shu Fang, Yanfeng Wang, and Cewu Lu. Transferable interactiveness knowledge for human-object interaction detection. In *Proceedings of the IEEE/CVF Conference on Computer Vision and Pattern Recognition*, pages 3585–3594, 2019.
- [31] Yue Liao, Si Liu, Fei Wang, Yanjie Chen, Chen Qian, and Jiashi Feng. Ppdm: Parallel point detection and matching for real-time human-object interaction detection. In *Proceedings of the IEEE/CVF Conference on Computer Vision and Pattern Recognition*, pages 482–490, 2020.
- [32] Miao Liu, Siyu Tang, Yin Li, and James M Rehg. Forecasting human-object interaction: joint prediction of motor attention and actions in first person video. In *European Conference on Computer Vision*, pages 704–721. Springer, 2020.
- [33] Shaowei Liu, Subarna Tripathi, Somdeb Majumdar, and Xiaolong Wang. Joint hand motion and interaction hotspots prediction from egocentric videos. In *Proceedings of the IEEE/CVF Conference on Computer Vision and Pattern Recognition*, pages 3282–3292, 2022.
- [34] Tianshan Liu and Kin-Man Lam. A hybrid egocentric activity anticipation framework via memory-augmented recurrent and one-shot representation forecasting. In *Proceedings of the IEEE/CVF Conference on Computer Vision and Pattern Recognition (CVPR)*, pages 13904–13913, June 2022.
- [35] Siyuan Brandon Loh, Debaditya Roy, and Basura Fernando. Long-term action forecasting using multi-headed attention-based variational recurrent neural networks. In *Proceedings of the IEEE/CVF Conference on Computer Vision and Pattern Recognition*, pages 2419–2427, 2022.
- [36] Joanna Materzynska, Tete Xiao, Roei Herzig, Huijuan Xu, Xiaolong Wang, and Trevor Darrell. Something-else: Compositional action recognition with spatial-temporal interaction networks. In *Proceedings of the IEEE/CVF Conference on Computer Vision and Pattern Recognition*, pages 1049–1059, 2020.
- [37] Antoine Miech, Ivan Laptev, Josef Sivic, Heng Wang, Lorenzo Torresani, and Du Tran. Leveraging the present to anticipate the future in videos. In *Proceedings of the IEEE Conference on Computer Vision and Pattern Recognition Workshops*, pages 0–0, 2019.
- [38] Kyle Min and Jason J Corso. Integrating human gaze into attention for egocentric activity recognition. In *Proceedings of the IEEE/CVF Winter Conference on Applications of Computer Vision*, pages 1069–1078, 2021.
- [39] Megha Nawhal, Akash Abdu Jyothi, and Greg Mori. Rethinking learning approaches for long-term action anticipation. In *European Conference on Computer Vision*, pages 558–576. Springer, 2022.
- [40] Yan Bin Ng and Basura Fernando. Forecasting future action sequences with attention: a new approach to weakly supervised action forecasting. *IEEE Transactions on Image Processing* 2020, 2020.
- [41] Yangjun Ou, Li Mi, and Zhenzhong Chen. Object-relation reasoning graph for action recognition. In *Proceedings of the IEEE/CVF Conference on Computer Vision and Pattern Recognition*, pages 20133–20142, 2022.
- [42] Mandela Patrick, Dylan Campbell, Yuki Asano, Ishan Misra, Florian Metze, Christoph Feichtenhofer, Andrea Vedaldi, and João F Henriques. Keeping your eye on the ball: Trajectory attention in video transformers. *Advances in neural information processing systems*, 34:12493–12506, 2021.
- [43] Zhaobo Qi, Shuhui Wang, Chi Su, Li Su, Qingming Huang, and Qi Tian. Self-regulated learning for egocentric video activity anticipation. *IEEE Transactions on Pattern Analysis and Machine Intelligence*, 2021.
- [44] Shaoqing Ren, Kaiming He, Ross Girshick, and Jian Sun. Faster r-cnn: Towards real-time object detection with region proposal networks. *Advances in neural information processing systems*, 28, 2015.
- [45] Cristian Rodriguez, Basura Fernando, and Hongdong Li. Action anticipation by predicting future dynamic images. In *Proceedings of the European Conference on Computer Vision (ECCV) Workshops*, pages 0–0, 2018.

- [46] Cristian Rodriguez, Basura Fernando, and Hongdong Li. Action anticipation by predicting future dynamic images. In *Proceedings of the European Conference on Computer Vision (ECCV) Workshops*, pages 0–0, 2018.
- [47] Debaditya Roy and Basura Fernando. Action anticipation using pairwise human-object interactions and transformers. *IEEE Transactions on Image Processing*, 30:8116–8129, 2021.
- [48] Debaditya Roy and Basura Fernando. Action anticipation using latent goal learning. In *Proceedings of the IEEE/CVF Winter Conference on Applications of Computer Vision (WACV)*, pages 2745–2753, January 2022.
- [49] Debaditya Roy and Basura Fernando. Predicting the next action by modeling the abstract goal. *arXiv preprint arXiv:2209.05044*, 2022.
- [50] Michael S Ryoo. Human activity prediction: Early recognition of ongoing activities from streaming videos. In *Proceedings of the International Conference on Computer Vision*, pages 1036–1043. IEEE, 2011.
- [51] Mohammad Sadegh Aliakbarian, Fatemeh Sadat Saleh, Mathieu Salzmann, Basura Fernando, Lars Petersson, and Lars Andersson. Encouraging lstms to anticipate actions very early. In *Proceedings of the IEEE International Conference on Computer Vision*, pages 280–289, 2017.
- [52] Fadime Sener, Dipika Singhania, and Angela Yao. Temporal aggregate representations for long-range video understanding. In *European Conference on Computer Vision*, pages 154–171. Springer, 2020.
- [53] Kevin Sexton, Amanda Johnson, Amanda Gotsch, Ahmed A Hussein, Lora Cavuoto, and Khurshid A Guru. Anticipation, teamwork and cognitive load: chasing efficiency during robot-assisted surgery. *BMJ quality & safety*, 27(2):148–154, 2018.
- [54] Behnam Sherafat, Changbum R Ahn, Reza Akhavian, Amir H Behzadan, Mani Golparvar-Fard, Hyunsoo Kim, Yong-Cheol Lee, Abbas Rashidi, and Ehsan Rezazadeh Azar. Automated methods for activity recognition of construction workers and equipment: State-of-the-art review. *Journal of Construction Engineering and Management*, 146(6):03120002, 2020.
- [55] Yao Teng, Limin Wang, Zhifeng Li, and Gangshan Wu. Target adaptive context aggregation for video scene graph generation. In *Proceedings of the IEEE/CVF International Conference on Computer Vision*, pages 13688–13697, 2021.
- [56] Ashish Vaswani, Noam Shazeer, Niki Parmar, Jakob Uszkoreit, Llion Jones, Aidan N Gomez, Łukasz Kaiser, and Illia Polosukhin. Attention is all you need. *Advances in neural information processing systems*, 30, 2017.
- [57] Carl Vondrick, Hamed Pirsiavash, and Antonio Torralba. Anticipating visual representations from unlabeled video. In *Proceedings of the IEEE Conference on Computer Vision and Pattern Recognition*, pages 98–106, 2016.
- [58] Boyu Wang, Lihan Huang, and Minh Hoai. Active vision for early recognition of human actions. In *Proceedings of the IEEE/CVF Conference on Computer Vision and Pattern Recognition*, pages 1081–1091, 2020.
- [59] Xiaolong Wang and Abhinav Gupta. Videos as space-time region graphs. In *Proceedings of the European conference on computer vision (ECCV)*, pages 399–417, 2018.
- [60] Chao-Yuan Wu, Yanghao Li, Karttikeya Mangalam, Haoqi Fan, Bo Xiong, Jitendra Malik, and Christoph Feichtenhofer. Memvit: Memory-augmented multiscale vision transformer for efficient long-term video recognition. In *Proceedings of the IEEE/CVF Conference on Computer Vision and Pattern Recognition*, pages 13587–13597, 2022.
- [61] Yu Wu, Linchao Zhu, Xiaohan Wang, Yi Yang, and Fei Wu. Learning to anticipate egocentric actions by imagination. *IEEE Transactions on Image Processing*, 30:1143–1152, 2021.
- [62] Olga Zatsarynna, Yazan Abu Farha, and Juergen Gall. Multi-modal temporal convolutional network for anticipating actions in egocentric videos. In *Proceedings of the IEEE/CVF Conference on Computer Vision and Pattern Recognition*, pages 2249–2258, 2021.
- [63] Aixi Zhang, Yue Liao, Si Liu, Miao Lu, Yongliang Wang, Chen Gao, and Xiaobo Li. Mining the benefits of two-stage and one-stage hoi detection. *Advances in Neural Information Processing Systems*, 34:17209–17220, 2021.
- [64] Chuhan Zhang, Ankush Gupta, and Andrew Zisserman. Is an object-centric video representation beneficial for transfer? *arXiv preprint arXiv:2207.10075*, 2022.
- [65] Tianyu Zhang, Weiqing Min, Jiahao Yang, Tao Liu, Shuqiang Jiang, and Yong Rui. What if we could not see? counterfactual analysis for egocentric action anticipation. In *IJCAI*, 2021.
- [66] Zeyun Zhong, David Schneider, Michael Voit, Rainer Stiefelhagen, and Jürgen Beyerer. Anticipative feature fusion transformer for multi-modal action anticipation. In *Proceedings of the IEEE/CVF Winter Conference on Applications of Computer Vision*, pages 6068–6077, 2023.